

See discussions, stats, and author profiles for this publication at: <https://www.researchgate.net/publication/272136805>

Solvothermal Synthesis of Hierarchical LiFePO₄ Microplates with Exposed (010) Faces as Cathode Materials for Lithium Ion Batteries

ARTICLE in INDUSTRIAL & ENGINEERING CHEMISTRY RESEARCH · AUGUST 2014

Impact Factor: 2.59 · DOI: 10.1021/ie501743b

CITATIONS

5

READS

23

6 AUTHORS, INCLUDING:



Weixin Zhang

Hefei University of Technology

105 PUBLICATIONS 2,512 CITATIONS

SEE PROFILE

Solvothermal Synthesis of Hierarchical LiFePO₄ Microplates with Exposed (010) Faces as Cathode Materials for Lithium Ion Batteries

Jun Zhang, Jianbo Lu, Doucheng Bian, Zeheng Yang,* Qing Wu, and Weixin Zhang*

School of Chemistry and Chemical Engineering, Hefei University of Technology and Anhui Key Laboratory of Controllable Chemical Reaction & Material Chemical Engineering, Anhui 230009, People's Republic of China

 Supporting Information

ABSTRACT: Hierarchical LiFePO₄ microplates have been synthesized by a solvothermal approach in ethanol solvent with self-prepared amorphous FePO₄ particles as precursors. The microplates expose a large scale of the (010) faces with a mean length of 2.5 μm, width of 1.5 μm and thickness of 200–500 nm. Furthermore, the hierarchical LiFePO₄ microplates are composed of nanosheets with a size of 50 nm and thickness of 10 nm. When the solvent ethanol was replaced by a mixture of water–ethanol (1/1, by volume) in the reaction, a distinctive morphology, the LiFePO₄ microflower, was obtained. After coating carbon, the LiFePO₄/C microplates deliver a high discharge capacity of 157 mAh g⁻¹ at 0.1 C, and exhibit excellent rate capability and cycling performance, which are much better than those for the LiFePO₄/C microflowers.

1. INTRODUCTION

Lithium ion batteries are considered to be the most promising candidate for electric vehicles (EVs) and hybrid EVs because of their high power densities compared to conventional rechargeable batteries.^{1,2} Olivine LiFePO₄ now stands as a competitive cathode material for next generation of green and sustainable lithium ion battery systems owing to its abundant resources, long life span, low toxicity, and high thermal stability.^{3–5} However, the capacity and rate performance of LiFePO₄ are seriously limited by the poor intrinsic electronic conductivity and the sluggish diffusion of lithium ions, which impedes battery applications.^{6,7}

During the past decades, various strategies have been adopted to surmount the inherent problems of LiFePO₄, such as coating with a thin electron-conducting layer,^{8–11} doping with foreign atoms,^{12–16} and decreasing the particle size.^{17–21} Fabricating hierarchical nano/microstructures is another approach because it can take advantage of both the nanosized building blocks and microsized assemblies.^{22–26} Guo et al.²³ presented a hydrothermal strategy to synthesize self-assembled LiFePO₄ nano/microspheres by using phytic acid as a novel phosphorus source, which achieved a discharge capacity of 155 mAh g⁻¹ at 0.1 C. In addition, it was certified recently that lithium ion conductivity can be improved by reducing the crystal size along the *b*-axis.²⁷ In our previous report,²⁸ we adopted a surfactant-assisted hydrothermal method to synthesize morphology-controlled LiFePO₄ (nanorods and nanoplates) with controllable *b*-axis thickness; the discharge capacity and rate performance have been found to increase with the decreasing thickness of the *b*-axis. Therefore, to synthesize a hierarchical structure composed of nanounits with a large *ac*-plane and a short *b*-axis is desirable. And such a strategy to improve the electrochemical performance of LiFePO₄ has attracted much attention recently.²⁹

Herein, we report a solvothermal approach to prepare hierarchical LiFePO₄ microplates assembled by nanosheets with self-prepared amorphous FePO₄ particles as precursors, and

specially, the nanosheets expose a large scale of (010) faces. As cathode materials for lithium ion batteries, the hierarchical LiFePO₄/C microplates composed of many nanosheets show enhanced electrochemical performance compared with the LiFePO₄/C microflowers that were obtained when the ethanol solvent was replaced by a mixed solvent of water–ethanol (1/1, by volume) in the reaction system.

2. EXPERIMENTAL SECTION

All chemicals were analytical grade from Sinopharm Chemical Reagent (China) Co., Ltd. and used as raw material without further purification.

2.1. Synthesis of Amorphous FePO₄ Particles. In a typical synthesis, 5.4 g of FeCl₃·6H₂O was dissolved in distilled water (80 mL), and 6.9 g of NH₄H₂PO₄ was added to the solution under vigorous stirring for 2 h. The resulting precipitates were collected by centrifugation, washed with distilled water and ethanol respectively for several times, and then dried at 65 °C for 5 h in air.

2.2. Synthesis of LiFePO₄ via a Solvothermal Method. 0.423 g of the amorphous FePO₄·2H₂O, 0.508 g of LiCl·H₂O, and 2 mL of N₂H₄·H₂O aqueous solution (1.6 M) were mixed in 40 mL of ethanol with stirring. Then the mixture was transferred to a 50 mL Teflon-lined stainless steel autoclave and placed in an oven at 180 °C for 24 h. After the product naturally cooled to ambient temperature, it was filtered, washed, and dried at 65 °C overnight.

2.3. Modification of LiFePO₄ with Carbon Coating. The LiFePO₄/C composites were made by postheat treatment. The as-synthesized LiFePO₄ was immersed in glucose solution (glucose/LiFePO₄ = 0.15:1 by weight ratio) to form a uniform slurry, and then dried at 80 °C for 12 h to remove the excess

Received: April 28, 2014

Revised: July 11, 2014

Accepted: July 17, 2014

Published: July 17, 2014



water. Then the sample was heated at 650 °C for 10 h in a tube furnace with N₂ atmosphere.

X-ray powder diffraction (XRD) tests were carried out on a Japan Rigaku D/max- γ B X-ray diffractometer with Cu K α radiation ($\lambda = 0.154\text{ }18\text{ nm}$), operated at 40 kV and 80 mA. Thermogravimetric analysis (TGA) was performed using a TG209F3 TGA/DTA instrument from room temperature to 800 °C at a heating rate of 10 °C min⁻¹ in air. Field-emission scanning electron microscopy (FESEM) measurement was carried out on a SU8020 field-emission scanning electron microscope, operated at an acceleration voltage of 5 kV. High resolution transmission electron microscopy (HRTEM) images were taken with a JEM-2100F transmission electron microscope, operated at an accelerating voltage of 200 kV.

The working electrodes were prepared by mixing 80 wt % of LiFePO₄/C, 15 wt % conducting carbon black, and 5 wt % of polyvinylidene fluoride (PVDF) in *N*-methyl-2-pyrrolidone (NMP) solvent. Then, the mixed slurry was cast onto a thin aluminum foil and evaporated at 65 °C for 5 h in air. After that, the cathode was roll-pressed and further dried in vacuum at 120 °C overnight. The liquid electrolyte was 1 M LiPF₆ dissolved in a mixed solution of ethylene carbonate (EC)/dimethyl carbonate (DMC) (1/1, by volume), and the separator was a Celgard 2400 microporous polypropylene membrane. All the cells (CR2032) were assembled in a dry argon-filled glovebox (both oxygen and water contents below 0.5 ppm) with lithium metal foil as the anode. The cells were charged at 0.5 C rate and discharged at different current rates over a voltage range of 2.0–4.2 V at room temperature on a multichannel battery tester (Neware Battery Testing System, Shenzhen Neware Electronic Co., China). The cyclic voltammetry (CV) measurements were carried out at a scanning rate of 0.1 mV s⁻¹ from 2.0 to 4.2 V (versus Li/Li⁺) at room temperature on a CHI604C electrochemical workstation (Shanghai Chenhua Instrument Co., China).

3. RESULTS AND DISCUSSION

The crystallinity of the as-prepared FePO₄ precursor was examined by powder XRD. As shown in Figure S1 (Supporting Information), the sample was expectedly amorphous in nature because the synthesis was carried out at room temperature. And the amorphous FePO₄ particles have a size distribution of about 60 nm, which can be observed from Figure S2 (Supporting Information).

It is generally acknowledged that iron phosphate typically contains some water molecules per unit cell. Therefore, thermogravimetric analysis was conducted to measure the amount of water of the amorphous FePO₄. Figure S3 (Supporting Information) shows the thermogravimetry results for a temperature variation from room temperature to 800 °C in air. A weight loss of about 18 wt % was observed, which corresponds to the content of two moles of water per mole of FePO₄, so the molecular formula should be written as FePO₄·2H₂O.

Figure 1 shows the XRD pattern of LiFePO₄ prepared in ethanol by solvothermal reaction. All the diffraction peaks can be indexed to an orthorhombic LiFePO₄ with *Pnma* space group (JCPDS No. 83-2092) without any observable impurity phase, such as Li₃PO₄ and Li₃Fe₂(PO₄)₃. After carbon coating, the obtained LiFePO₄/C composite still maintains the LiFePO₄ phase. It is worth noting that the peak around 30° ((020) face or (211) face) shows a predominant intensity compared with other peaks, implying possible oriented growth of the LiFePO₄

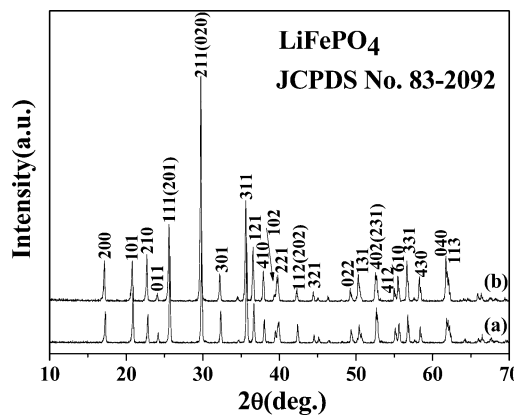


Figure 1. XRD patterns of LiFePO₄ prepared in ethanol by (a) solvothermal reaction and (b) after carbon coating.

crystals. In addition, there are no additional diffraction peaks associated with carbon generated from glucose, which indicates that the formed carbon is probably amorphous.

Figure 2 displays the FESEM (a, b, c, d) images and HRTEM (e, f) images of the LiFePO₄/C sample. The FESEM images in Figure 2a,b show that the as-prepared product consists of numerous microplates with a mean length of 2.5 μm, width of 1.5 μm, and thickness of 200–500 nm. High magnification FESEM images in Figure 2c,d give more detailed information. The hierarchical microplates are composed of many nanosheets with a mean size of 50 nm and thickness of about 10 nm. Figure 2e shows the HRTEM image of a nanosheet of LiFePO₄/C. The inserted selected area electron diffraction (SAED) pattern viewed along the [010] zone axis implies its single crystalline nature. HRTEM image in Figure 2f (corresponding to the area marked by a circle in Figure 2e) shows that the lattice interplanar spacings of 0.51 and 0.23 nm correspond to the (200) and (002) planes of orthorhombic LiFePO₄, respectively, indicating that the large plane of the LiFePO₄/C microplate lies in the *ac*-plane, viewed along the *b*-direction. The preferential (010) plane is consistent with the above XRD patterns (Figure 1), in which the (020) peak shows unusually high intensity. In addition, Figure 2f shows uniform carbon coating (amorphous region) with a thickness of about 4 nm on the surface of the LiFePO₄/C nanosheet.

When ethanol was replaced by the mixed solvent of water–ethanol (1/1, by volume) in the solvothermal reaction and the other reaction conditions were the same, LiFePO₄ microflowers, instead of microplates, were obtained. Figure 3 shows the structure and morphology of LiFePO₄/C microflowers prepared in the mixed solvent. The average size of the microflowers is about 8 μm, and they are composed of many rhombus-shaped blocks with a mean length of 6 μm and thickness of 1 μm.

The contents of carbon in LiFePO₄/C microplates and LiFePO₄/C microflowers were measured using a carbon sulfur automatic analyzer (HH2000A, Wuxi Chuangxiang Co., China), and the values are 3.41 and 3.45 wt %, respectively.

On the basis of the above observation, we postulate that the formation of LiFePO₄ in our experiment is based on a dissolution–recrystallization process.²² With the temperature increasing steadily during solvothermal reaction, the solid precursors dissolve and form LiFePO₄ crystal nuclei. And in our case, ethanol may prefer to adsorb on the (010) plane and tune the preferential growth of LiFePO₄ crystals along [200] and

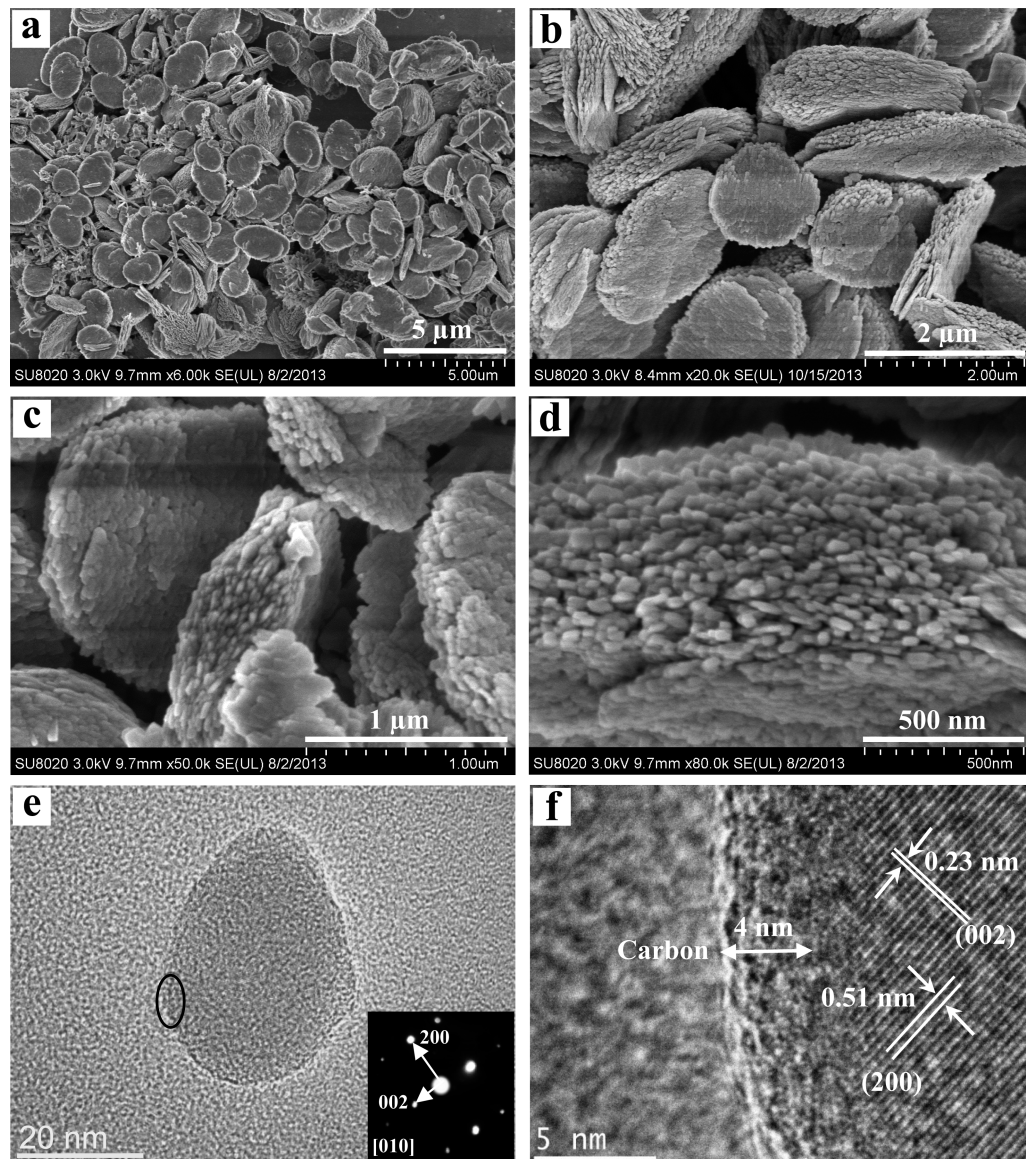


Figure 2. FESEM (a, b, c, d) images of LiFePO₄/C microplates and HRTEM images of the whole (e) and a part (f) of a LiFePO₄/C nanosheet; inset in panel e: selected area electron diffraction (SAED) pattern.

[002], leading to formation of the nanosheets with a large scale of (010) faces. According to published literature,³⁰ the surface energy of the (010) plane is less than that of the (001) and (100) planes in olivine LiFePO₄. As the reaction proceeds, the nanosheets agglomerate along the (001) and (100) planes for minimizing the surface energy. Finally, they transform to microplates through an orientation attachment.

However, adding water into the solvothermal reaction medium raises the solubility of the precursors, the supersaturation degree of the solution becomes lower under hydrothermal conditions, and nucleation rate is therefore decreased. Meanwhile, as the ethanol concentration decreases, the adsorption of ethanol molecules on LiFePO₄ crystal plane is not strong enough to suppress the nuclei growth. As a result, the crystal nuclei grow into larger LiFePO₄ particles, as shown in Figure S4a (Supporting Information). And then they transform to rhombus-shaped blocks via a process known as Ostwald ripening (smaller crystallites would dissolve into solution and eventually regrow into larger crystals, as shown in Figure S4b (Supporting Information)). Finally, they assembled

into microflowers, as shown in Figure S4c,d (Supporting Information). A similar phenomenon has been observed in previous reports.^{31,32}

In addition, we did a magnified experiment by increasing the starting materials by 5 times in a 50 mL Teflon-lined stainless steel autoclave. As shown in Figure S5 (Supporting Information), as the concentration of the starting materials is increased by 5 times for the same amount of ethanol solvent, the obtained sample exists in a mixture of hierarchical microplates and nanorods. It can be seen that a large portion of the product still takes the hierarchical microplate morphology, but some exist in a nanorod morphology. This is because the relative amount of ethanol molecules adsorbing on the LiFePO₄ crystals decreases as the concentration of the starting materials is increased by 5 times, leading to suppressing effect on the nuclei growth is not strong enough to obtain homogeneous LiFePO₄ hierarchical microplates.

The electrochemical performance of the LiFePO₄/C samples has been investigated. The LiFePO₄/C microflowers were also modified with carbon coating under the same conditions for

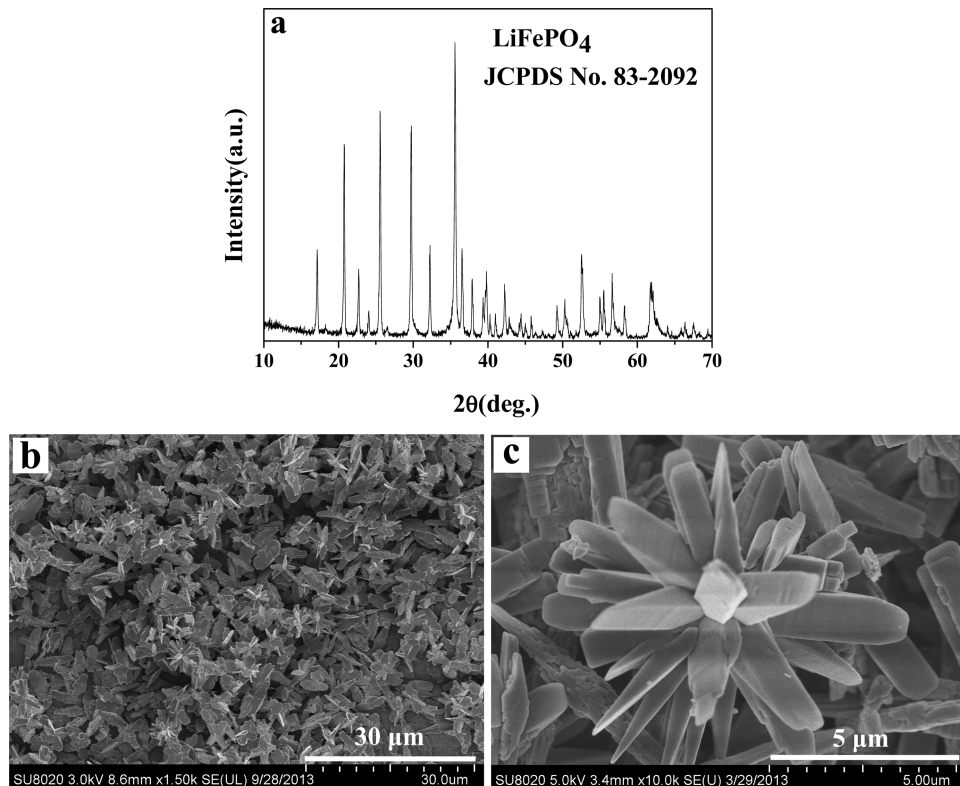


Figure 3. Structure and morphology of LiFePO₄/C microflowers prepared in the water–ethanol mixed solvent; (a) XRD pattern and (b, c) FESEM images.

LiFePO₄/C microplates. Figure 4 exhibits the typical charge/discharge voltage profiles of the two LiFePO₄/C samples with current density varying from 0.1 C (17 mA g^{-1}) to 20 C ($3,400 \text{ mA g}^{-1}$). The LiFePO₄/C microplates deliver an initial discharge capacity of 157 mAh g^{-1} at 0.1 C, even the current density is increased to 10 and 20 C, they can also deliver discharge capacities of 100 and 81 mAh g^{-1} , respectively. While the LiFePO₄/C microflowers not only deliver lower initial discharge capacity of 144 mAh g^{-1} at 0.1 C, but also exhibit obvious capacity fading and enormous polarization with increasing discharge rate and their discharge capacity is reduced to 27 mAh g^{-1} at 20 C.

Figure 5 further compares the rate performance of the two LiFePO₄/C samples. It can be observed clearly that the LiFePO₄/C microplates show much slower capacity decay than the LiFePO₄/C microflowers, especially at high rates. When the current rate is decreased from 20 C back to 0.1 C, the discharge capacities are restored to 99.1% and 97.4% of their initial capacities, respectively. Compared with LiFePO₄/C microflowers, LiFePO₄/C microplates show better capability. Furthermore, the LiFePO₄/C microplates exhibit superior cycling performance. As shown in Figure 6, the reversible discharge capacity remains approximately 139 and 118 mAh g^{-1} without obvious capacity fading after 100 cycles at 1 and 5 C, respectively.

A cycling voltammogram (CV) test was also carried out to investigate the influence of morphology on the electrochemical properties. The two LiFePO₄/C samples were tested at a scanning rate of 0.1 mV s^{-1} between the voltage limits of 2.5 and 4.2 V (versus Li⁺/Li) and their CV profiles are shown in Figure 7. The LiFePO₄/C microplates exhibit an anodic peak at 3.54 V and a corresponding cathodic response at 3.33 V. The

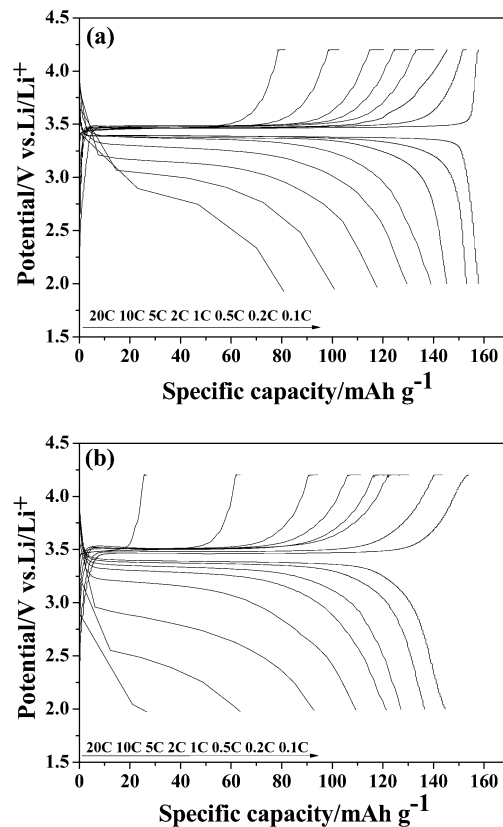


Figure 4. Charge–discharge profiles of LiFePO₄/C samples at different discharge rates for (a) microplates and (b) microflowers.

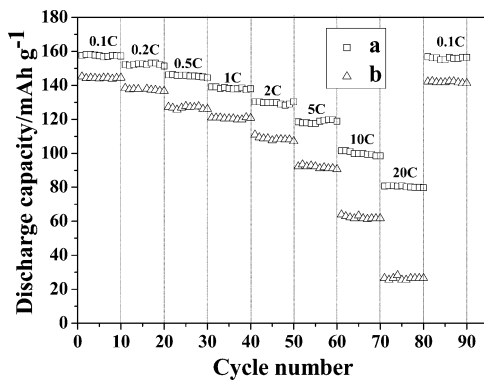


Figure 5. Rate performance of the LiFePO_4/C samples for (a) microplates and (b) microflowers.

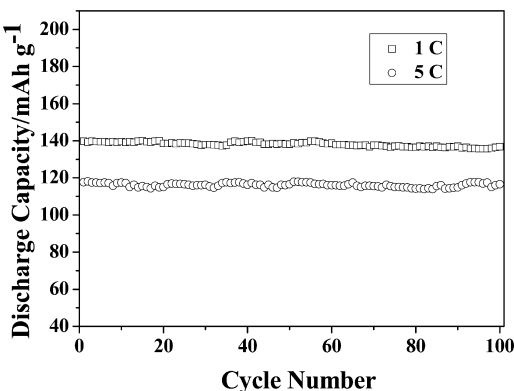


Figure 6. Cycling performance of LiFePO_4/C microplates at 1 and 5 C.

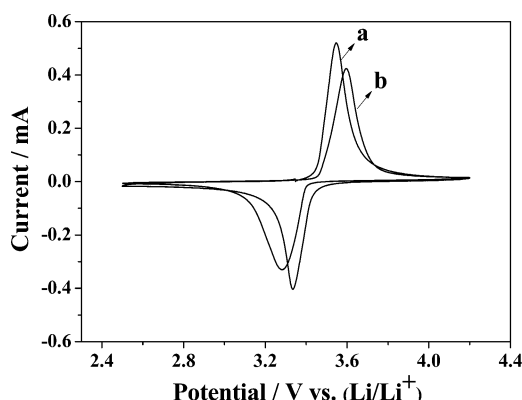


Figure 7. Cycling voltammograms for LiFePO_4/C samples at a scan rate of 0.1 mV s^{-1} between 2.5 and 4.2 V for (a) microplates and (b) microflowers.

separation potential of LiFePO_4/C microplates is 0.21 V, whereas that of LiFePO_4/C microflowers is 0.32 V. The more symmetric and spiculate peak profile for LiFePO_4/C microplates indicates a better reversible electrochemical reaction during lithium ion insertion and extraction.³³

Electrochemical impedance spectroscopy was performed in the full charge state. Figure 8 shows Nyquist plots of the two LiFePO_4/C samples. The intercept on the real axis in high frequency corresponds to the solution resistance (R_e). The semicircle in the middle frequency range indicates the charge transfer resistance (R_{ct}). As shown in Figure 8, both LiFePO_4/C samples exhibit similar R_e , whereas the R_{ct} of the LiFePO_4/C microflowers is larger than that of the LiFePO_4/C microplates.

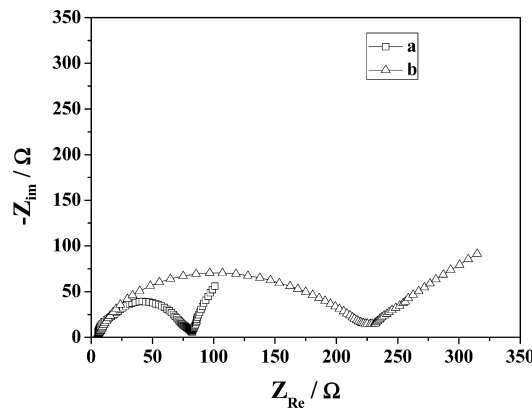


Figure 8. Electrochemical impedance spectroscopy results of LiFePO_4/C samples at full charge in the frequency range between 100 kHz and 10 mHz for (a) microplates and (b) microflowers.

microplates (82.3Ω) is much smaller than that of the LiFePO_4/C microflowers (227.7Ω). This indicates that the conductivity of the LiFePO_4/C microplates is much higher, which is beneficial to the kinetic behavior during charge and discharge process.³⁴

According to the above discussion, the LiFePO_4/C microplates show superior electrochemical performance, which can be mainly attributed to the following reasons. First, the hierarchical LiFePO_4/C microplates with nanosheet building blocks expose a large scale of the (010) faces, which is active for lithium ion intercalation/extraction.³⁵ Second, the nanosized building blocks can decrease the lithium ion migration length and improve the kinetics of LiFePO_4 . Third, the voids between the LiFePO_4 nanosheets can allow for better infiltration of the electrolyte and facilitate the diffusion of lithium ions. Fourth, the homogeneous carbon-coating layer can enhance the electronic conductivity of LiFePO_4 .

4. CONCLUSION

In summary, we demonstrated an effective solvothermal route to preparation of hierarchical LiFePO_4 microplates that are composed of many ultrathin nanosheets with large exposure of the (010) face. When ethanol was replaced by the water–ethanol mixed solvent (1/1, by volume) in the solvothermal reaction, LiFePO_4 microflowers were obtained. After carbon coating, the LiFePO_4/C microplates show better electrochemical performance compared with the LiFePO_4/C microflowers. The former exhibits low polarization and a high reversible specific capacity of 157 mAh g^{-1} at 0.1 C, as well as excellent rate capability and cycling performance. The superior properties of the LiFePO_4/C microplates can be attributed to the hierarchical plate-like structure with nanosheet building blocks, which possess a large *ac*-plane and a short *b*-axis. Besides, the homogeneous carbon coating also contributes to enhance their performance.

ASSOCIATED CONTENT

S Supporting Information

XRD pattern, FESEM image and thermogravimetric measurement of FePO_4 sample, and the assembling process of LiFePO_4 microflowers. This material is available free of charge via the Internet at <http://pubs.acs.org>.

AUTHOR INFORMATION

Corresponding Authors

*Weixin Zhang. Tel: +86-551-62901450. Fax: +86-551-62901450. E-mail: wxzhang@hfut.edu.cn.
*Zeheng Yang. Tel: +86-551-62901450. Fax: +86-551-62901450. E-mail: yangzh0219@sina.com.

Notes

The authors declare no competing financial interest.

ACKNOWLEDGMENTS

This work was supported by the National Natural Science Foundation of China (NSFC Grants 20976033, 21176054 and 21271058), the Fundamental Research Funds for the Central Universities (2010HGZY0012) and the Education Department of Anhui Provincial Government (TD200702).

REFERENCES

- (1) Goodenough, J. B. Rechargeable batteries: Challenges old and new. *J. Solid State Electrochem.* **2012**, *16*, 2019–2029.
- (2) Li, H.; Wang, Z.; Chen, L.; Huang, X. Research on advanced materials for Li-ion batteries. *Adv. Mater.* **2009**, *21*, 4593–4607.
- (3) Lyczko, N.; Nzihou, A.; Sharrock, P.; Germeau, A.; Toussaint, C. Characterization of LiFePO₄/C cathode for lithium ion batteries. *Ind. Eng. Chem. Res.* **2012**, *51*, 292–300.
- (4) Yamada, A.; Chung, S. C.; Hinokuma, K. Optimized LiFePO₄ for lithium battery cathodes. *J. Electrochem. Soc.* **2001**, *148*, A224–A229.
- (5) Wang, Y. G.; He, P.; Zhou, H. S. Olivine LiFePO₄: Development and future. *Energy Environ. Sci.* **2010**, *4*, 805–817.
- (6) Huang, Y. H.; Goodenough, J. B. High-Rate LiFePO₄ lithium rechargeable battery promoted by electrochemically active polymers. *Chem. Mater.* **2008**, *20*, 7237–7241.
- (7) Liu, Y.; Cao, C.; Li, J. Enhanced electrochemical performance of carbon nanospheres–LiFePO₄ composite by PEG based sol–gel synthesis. *Electrochim. Acta* **2010**, *55*, 3921–3926.
- (8) Prosini, P. P.; Lisi, M.; Zane, D.; Pasquali, M. Determination of the chemical diffusion coefficient of lithium in LiFePO₄. *Solid State Ionics* **2002**, *148*, 45–51.
- (9) Kong, L. B.; Zhang, P.; Liu, M. C.; Liu, H.; Luo, Y. C.; Kang, L. Fabrication of promising LiFePO₄/C composite with a core–shell structure by a moderate in situ carbothermal reduction method. *Electrochim. Acta* **2012**, *70*, 19–24.
- (10) Wang, K.; Cai, R.; Yuan, T.; Yu, X.; Ran, R.; Shao, Z. P. Process investigation, electrochemical characterization and optimization of LiFePO₄/C composite from mechanical activation using sucrose as carbon source. *Electrochim. Acta* **2009**, *54*, 2861–2868.
- (11) Wang, Y. G.; Wang, Y. R.; Hosono, E. J.; Wang, K. X.; Zhou, H. S. The design of a LiFePO₄/carbon nanocomposite with a core–shell structure and its synthesis by an in situ polymerization restriction method. *Angew. Chem., Int. Ed.* **2008**, *47*, 7461–7465.
- (12) Moskon, J.; Dominko, R.; Korosec, R. C.; Gaberscek, M.; Jamnik, J. Morphology and electrical properties of conductive carbon coatings for cathode materials. *J. Power Sources* **2007**, *174*, 683–688.
- (13) Pei, B.; Wang, Q.; Zhang, W. X.; Yang, Z. H.; Chen, M. Enhanced performance of LiFePO₄ through hydrothermal synthesis coupled with carbon coating and cupric ion doping. *Electrochim. Acta* **2011**, *56*, 5667–5672.
- (14) Gao, H. Y.; Jiao, L. F.; Yang, J. Q.; Qi, Z.; Wang, Y. J.; Yuan, H. T. High rate capability of Co-doped LiFePO₄/C. *Electrochim. Acta* **2013**, *97*, 143–149.
- (15) Meethong, N.; Kao, Y. H.; Speakman, S. A.; Chiang, Y. M. Aliovalent doping for improved battery performance: Aliovalent substitutions in olivine lithium iron phosphate and impact on structure and properties. *Adv. Funct. Mater.* **2009**, *19*, 1060–1070.
- (16) Hong, J.; Wang, C. S.; Kasavajjula, U. Kinetic behavior of LiFeMgPO₄ cathode material for Li-ion batteries. *J. Power Sources* **2006**, *162*, 1289–1296.
- (17) Fang, X. S.; Li, J.; Huang, K. L.; Liu, S. Q.; Huang, C. H.; Zhuang, S. X.; Zhang, J. B. Synthesis and electrochemical properties of K-doped LiFePO₄/C composite as cathode material for lithium-ion batteries. *J. Solid State Electrochem.* **2012**, *16*, 767–773.
- (18) Weng, S. Y.; Yang, Z. H.; Wang, Q.; Zhang, J.; Zhang, W. X. A carbothermal reduction method for enhancing the electrochemical performance of LiFePO₄/C composite cathode materials. *Ionics* **2013**, *19*, 235–243.
- (19) Wang, Y.; Wang, J.; Yang, J.; Nuli, Y. High-rate LiFePO₄ electrode material synthesized by a novel route from FePO₄·4H₂O. *Adv. Funct. Mater.* **2006**, *16*, 2135–2141.
- (20) Rangappa, D.; Sone, K.; Ichihara, M.; Kudo, T.; Honma, I. Rapid one-pot synthesis of LiMPO₄ (M=Fe, Mn) colloidal nanocrystals by supercritical ethanol process. *Chem. Commun.* **2010**, *46*, 7548–7550.
- (21) Fey, G. T. K.; Tu, H. J.; Huang, K. P.; Lin, Y. C.; Kao, H. M.; Chan, S. H. Particle size effects of carbon sources on electrochemical properties of LiFePO₄/C composites. *J. Solid State Electrochem.* **2012**, *16*, 1857–1862.
- (22) Tang, J. L.; Zhao, H. P.; Li, G. F.; Lu, Z.; Xiao, S. Q.; Chen, R. Citrate/urea/solvent mediated self-assembly of (BiO)₂CO₃ hierarchical nanostructures and their associated photocatalytic performance. *Ind. Eng. Chem. Res.* **2013**, *52*, 12604–12612.
- (23) Su, J.; Wu, X. L.; Yang, C. P.; Lee, J. S.; Kim, J.; Guo, Y. G. Self-Assembled LiFePO₄/C nano/microspheres by using phytic acid as phosphorus source. *J. Phys. Chem. C* **2012**, *116*, 5019–5024.
- (24) Wang, Q.; Zhang, W. X.; Yang, Z. H.; Weng, S. Y.; Jin, Z. J. Solvothermal synthesis of hierarchical LiFePO₄ microflowers as cathode materials for lithium ion batteries. *J. Power Sources* **2011**, *196*, 10176–10182.
- (25) Lan, S.; Liu, L.; Li, R. Q.; Leng, Z. H.; Gan, S. C. Hierarchical hollow structure ZnO: Synthesis, characterization, and highly efficient adsorption/photocatalysis toward congo red. *Ind. Eng. Chem. Res.* **2014**, *53*, 3131–3139.
- (26) Sun, C. W.; Rajasekharan, S.; Goodenough, J. B.; Zhou, F. Monodisperse porous LiFePO₄ microspheres for a high power Li-ion battery cathode. *J. Am. Chem. Soc.* **2011**, *133*, 2132–2135.
- (27) Nan, C. Y.; Lu, J.; Li, L. H.; Li, L. L.; Peng, Q.; Li, Y. D. Size and shape control of LiFePO₄ nanocrystals for better lithium ion battery cathode materials. *Nano Res.* **2013**, *6*, 469–477.
- (28) Pei, B.; Yao, H. X.; Zhang, W. X.; Yang, Z. H. Hydrothermal synthesis of morphology-controlled LiFePO₄ cathode material for lithium-ion batteries. *J. Power Sources* **2012**, *220*, 317–323.
- (29) Jiang, Y. M.; Liao, S. J.; Liu, Z. S.; Xiao, G.; Liu, Q. B.; Song, H. Y. High performance LiFePO₄ microsphere composed of nanofibers with an alcohol-thermal approach. *J. Mater. Chem. A* **2013**, *1*, 4546–4551.
- (30) Wang, L.; Zhou, F.; Meng, Y. S.; Ceder, G. First-principles study of surface properties of LiFePO₄: Surface energy, structure, wulff shape, and surface redox potential. *Phys. Rev. B* **2007**, *76*, 165435.
- (31) Wang, X. B.; Cai, W. P.; Lin, Y. X.; Wang, G. Z.; Liang, C. H. Mass production of micro/nanostructured porous ZnO plates and their strong structurally enhanced and selective adsorption performance for environmental remediation. *J. Mater. Chem.* **2010**, *20*, 8582–8590.
- (32) Qin, X.; Wang, X. H.; Xiang, H. M.; Xie, J.; Li, J. J.; Zhou, Y. C. Mechanism for hydrothermal synthesis of LiFePO₄ platelets as cathode material for lithium-ion batteries. *J. Phys. Chem. C* **2012**, *114*, 16806–16812.
- (33) Jiang, Z. Q.; Jiang, Z. J. Effects of carbon content on the electrochemical performance of LiFePO₄/C core/shell nanocomposites fabricated using FePO₄/polyaniline as an iron source. *J. Alloys Compd.* **2012**, *537*, 308–317.
- (34) Shi, Z. Q.; Huang, M.; Yang, K.; Hu, X. B.; Tan, B.; Huang, X. L.; Den, Z. H. Effect of synthesis temperature and molar ratio of organic lithium salts on the properties and electrochemical performance of LiFePO₄/C composites. *J. Solid State Electrochem.* **2012**, *16*, 811–818.

(35) Nan, C. Y.; Lu, J.; Chen, C.; Peng, Q.; Li, Y. D. Solvothermal synthesis of lithium iron phosphate nanoplates. *J. Mater. Chem.* **2011**, *21*, 9994–9996.